## Application of the Biris Range Sensor for Volume Evaluation

Blais, François; Lecavalier, M.



**Publisher's version / Version de l'éditeur:**
https://doi.org/10.4224/8914033
*Proceedings of the Optical 3-D Measurement Techniques III, 1995*

**APPLICATION OF THE BIRIS RANGE SENSOR FOR VOLUME EVALUATION**

F. Blais, M. Lecavalier, J.-A. Beraldin
National Research Council Canada
Institute for Information Technology
Ottawa, Ontario, Canada, K1A-0R6

## Abstract

This paper describes recent improvements to the Biris optical range sensor and the application of the technology for the estimation of volume with emphasis on wood volume measurement. A description of the range sensor and the algorithms used to calculate the volume from range data are given. Two techniques are presented: 1) evaluation of volume using model fit, and, 2) evaluation of volume directly from raw range data.

## 1. Introduction

Because of its vast territory and large natural resources, Canada's primary industries occupy a very important place in its economy. The exploitation of its primary resources plays a vital role and volume measurement, used to decide the stumpage payments to governments and producers and to monitor production quality and quantity, is an integral part of any harvesting operation. Since licence holders are accountable for scaling, it has become a quest to maximize accuracy at minimum cost. The techniques currently in use involve the establishment of representative samples' plans, volume tables, and weight-to-volume ratios.

Sources of scaling errors manifest themselves in two forms: administrative and structural errors. Administrative errors are difficult to quantify and result from faulty planning, human error, or a mixture of both. The common causes are failure to meet successfully sampling requirements, the use of population statistics to calculate volumes of unrepresentative sample, or the use of outdated statistics.[1,2,3] Structural type errors are built into the measurement methodology. They are mainly caused by quantization methods used to simplify the work procedure. For example for wood, dividing the logs into fixed 2-cm diameter and length classes introduce log volume measurements that can vary from -13% to +14% within a given diameter class.[4] Although some of these variations usually cancel out with large samples, other errors such as diameter measurement using calipers, diameter tapes, or delimber arms in processors, tends to overestimate volumes and creates cumulative bias.[1,4,5]

Benefits stemming from automated volume measurement procedures and increased accuracy are, first and foremost cost reduction, improved control and planning, better optimization in the production and thus reduced waste. In the long term, shape measurements have the potential of providing characteristics that industry can use to plan their production schedule "just in time." For example, to detect how many oversized pieces can potentially jam debarkers or conveyer belts and the adjustments needed for optimal performances.

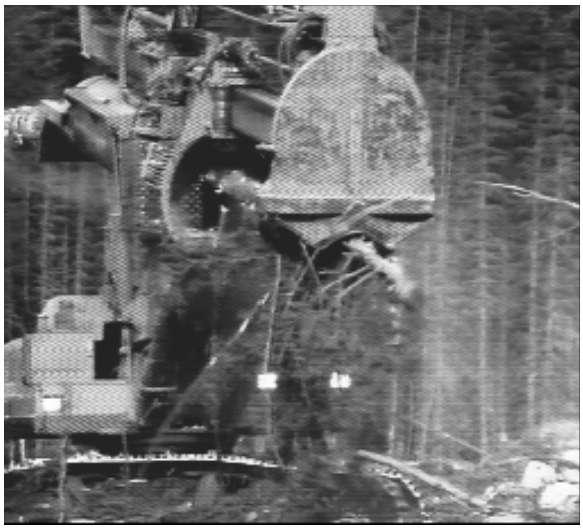

**Figure 1**. Delimber machine in wood harvesting.

In this paper a description of the range sensor used for the experiment, a definition of the algorithms developed for the evaluation of the cross-section of logs, and some experimental results are presented. Because of the length of the paper, emphasis is placed on the radial measurement of logs volume as it is generally encountered on a delimber machine (Fig. 1). Even though works have been done to extract the volume of multiple logs simultaneously, only single log measurements will be presented.

## 2. The Optical Range Sensor

One main advantage of an optical system lies in its capabilities of obtaining information and measurements without having to be physically in contact with the object under inspection. In

that respect, optical range sensors have the extra advantage, over conventional imaging devices, of directly providing the information about the shape and dimensions of the object with a minimum of computer processing and therefore reducing the complexity and cost of a system and increasing its reliability.

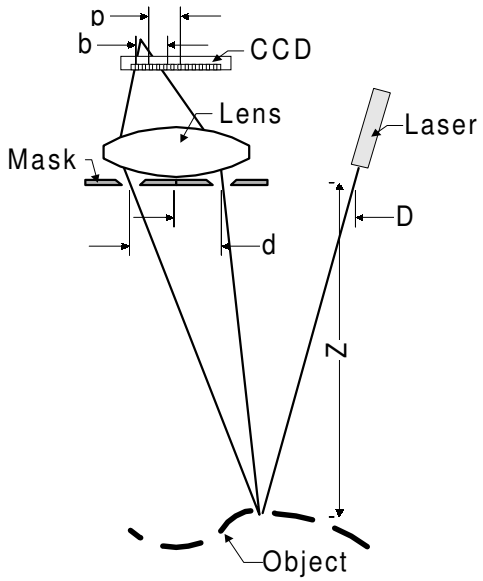


**Figure 2**: Optical geometry of the Biris sensor.

The Biris range sensor has been developed to work in difficult environments where reliability, robustness, and ease of maintenance are important.[6] The optical principle of the Biris technique is shown in Figure 2. The range sensor consists basically of a mask with two apertures, a camera lens, and a standard solid state compact video camera. The double aperture mask replaces the iris of a standard camera lens (thus the name bi-iris). Produced by a solid state laser diode, one to three laser lines are projected on the object and a double image of the projected line or lines is measured on the CCD video camera. Range is obtained by measuring both the separation $b$ of each pair of imaged lines and their centre position $p$ using:

$$z = \left[\psi\left(l^{-1} - \frac{l-f}{fdl}\,b\right) + (1-\psi)\left(\frac{\tan\vartheta}{D} - \frac{l-f}{fDl}\,p\right)\right]^{-1} \qquad \textbf{(1)}$$

where $f$ is the focal length of the lens, $l$ is the distance between a theoretical reference plane and the lens, $d$ is the separation between the two apertures, $D$ is the laser-lens separation, $\vartheta$ is the laser projector angle, and $\psi$ is the relative $b$-$p$ contribution ratio.

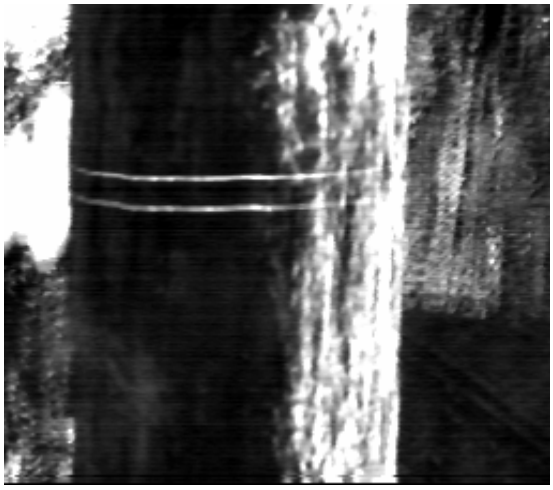

**Figure 3**: Video image of a log as seen by Biris sensor.

The method combines two different range measurement techniques in a single camera. Immunity to ambient illumination (such as sun interferences) and false detections is obtained by the use of special video image processing algorithms that extract the laser peaks in real-time, and by the range measurement redundancy

obtained from the two conditions ψ=0 and ψ=1, i.e. from equation (1), $Z_{(\psi=0)} = Z_{(\psi=1)}$. Any point not satisfying this condition is considered a false measurement and rejected. Fig. 3 shows a typical Biris image obtained on a delimber machine. The effects of ambient illumination created by the sun, though an optical interference filter was used, are still present. The double aperture mask creates a doubled image of both the laser line and the background.

The video processing algorithms are implemented on two PC-AT compatible modules occupying two slots on the PC backplane. The Video Digitization Boards (VDB) contains a 12-bits A/D converter running at 10 MHZ for increased video signal dynamic range. The Digital Processing Board (DPB) contains the video memory, the sub-pixel laser line detection module, and two T805 Inmos Transputers for signal conditioning, calibration, and system control. Each Biris processor can interface to four cameras, each camera being able to acquire multiple laser lines projected simultaneously on the object. The maximum capacity of the system depends on the number of slots available on the PC-AT bus. Fig. 4 shows a 486 ruggedized portable unit developed at NRC. Characteristics are summarized in Tables 1 and 2. It is worth


**Figure 4**: Biris processing unit and camera head.

| | |
|---|---|
| Points / profile | 256 |
| Field of view | 30 deg |
| Range accuracy (RMS) | 0.2 mm @ 0.3 m<br>1 mm @ 0.6 m<br>2 mm @ 0.9 m<br>3 mm @ 1.2 m |
| Depth of field | 0.3 m to >2 m |
| Dimensions | 15 × 12 × 6 cm |
| Weight | <1 kg |
| Power Supply | 12 V / 0.4 A |

**Table 1**: Characteristics of the Biris camera Head

| | |
|---|---|
| Processor | PC-AT comp. 486-66 |
| Memory | 8 Meg Ram - 512 Meg Disk |
| Operating System | DOS + Windows 3.1 |
| Display | VGA - LCD |
| Dimensions | 36 cm × 22 cm × 16 cm |
| Maximum Rating | 120-240V (60-50 Hz) |

**Table 2**: Characteristics of the Processor System

mentioning here that range accuracy is dependent on the camera head geometry and the focal length of the lens. It is possible to obtain different characteristics of accuracy and field of view if a different head is used.

## 3. Volume measurement

Let assume that $f(x,y,z)$ is a function describing the surface of the object that can be either a geometric model or simply the range data themselves acquired by the sensor. Then the volume is obtained by evaluating the double integral:

$$V = \iint f(x,y)\ dx\ dy \qquad \textbf{(2)}$$

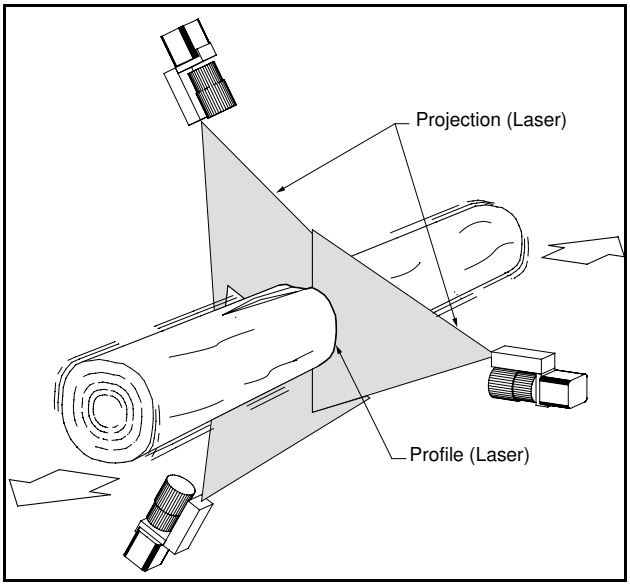


**Figure 5** Principle of radial measurement using one, two, or three sensors.

As shown in Fig. 5, a curtain of light is projected on the object to measure the cross section. While the range sensor acquires the -$X$ and -$Z$ coordinates of the surface of the object, the -$Y$ coordinate must be obtained, either by the mechanical displacement of the object while the object is being processed (e.g., conveyer belt, delimber), or using another range sensor along the displacement axis -$Y$. In this later case, the laser line is projected parallel to the displacement and inter-correlation between successive profiles provides the relative displacement $\Delta y$ between sequential video frames.

In the digital domain, equation (2) is rewritten:

$$V = \sum\sum f(x,y)\ \Delta x\ \Delta y = \sum S\ \Delta y \qquad \textbf{(3)}$$

In practice, two different techniques can be used to evaluate the cross section surface $S$ of material:

1) The fitting of a model of the object and the evaluation of the volume from it are preferred when:

- only a partial view or section of the object can be measured, the model infers the whole object shape from this partial measurement;

- data are noisy or corrupted by other objects (e.g., flying debris) creating important outliers in the data;
- the object can be described by a simple geometrical model.

2) The computation of volume from the raw data using equation (3) when:
- a complete view of the object is available;
- only partial views are available but the missing views can be estimated easily (e.g., on a conveyer belt, the conveyer belt is first measured empty).

Fig. 5 illustrates the notion of radial log measurement used in this paper, with one or two Biris cameras to obtain only a partial section of the log, or three cameras to cover the full cross section. Other possible uses of the sensor include: 1) volume measurement of raw material on a conveyer belt, and, 2) wood volume evaluation using axial measurements of logs, for example to measure a pile of wood or truck load. In the first case objects can have any shape and therefore raw data volume computation will be preferred; in the later both techniques can be used.

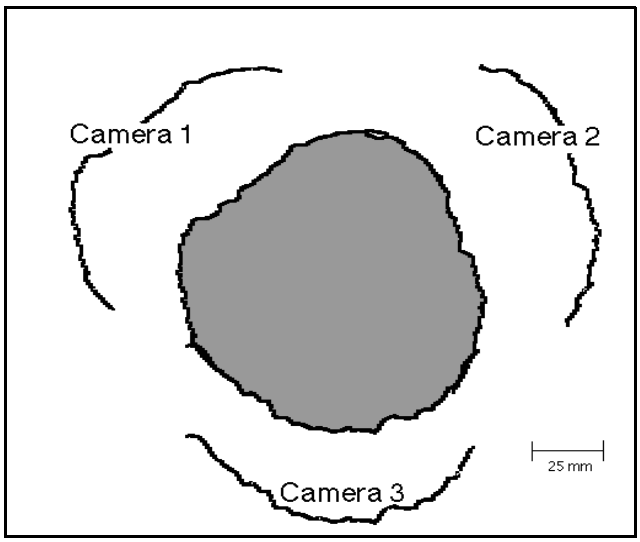


**Figure 6**: Raw data and cross section of one of the log sample showing its irregular shape.

This paper assumes that the cameras, when multiple cameras are used, are properly registered. Camera registration consists of evaluating the coordinate transformation matrix (yaw-pitch-roll-x-y-z) needed to have the measurements, from each camera, all in the same *-u,-v,-w* coordinate system. Fig. 6 shows the result of acquiring the cross-section of a single log. The raw data, shown for each camera, have been properly registered.

## 4. Volume measurement using a model

In Canada, current measurement techniques modelize the log with a cylinder of diameter $D_1$ and $D_2$ at each extremity of a tree of length $L$. The volume is $V=\pi \left( D_1^2+D_2^2 \right) L/8$. To be consistent with current scaling techniques that classify the trees in diameter classes, this paper uses the equivalent diameter $D$ of the log as reference for comparison. The experiment consisted of acquiring the diameter of one or several logs simultaneously using one, two, or

three Biris cameras to test different possible configurations of the sensors and their effects on the measurements. The three cameras are mounted at 120° to each other to cover most of the cross section of the object. Total volume is obtained by moving the sensor along the length of the log and accumulating the different cross sections of length $\Delta L$ between profiles using:

$$V = \sum S_j \, \Delta L_j, \qquad S_j = \frac{\pi}{4} D_j^2 \tag{4}$$

### *4.1 Circle*

Because of the roughness of "natural" objects, the distortion in their shapes (not being a perfect circle), and the accuracy of the range data, a 3-D measurement $u_i, v_i$ on the surface of the object will produce an error $\varepsilon_i$. This error $\varepsilon_i$ and the equation of a circle of centre $u_o, v_o$ and radius $r$, yields:

$$\begin{aligned} \epsilon_i &= \left( u_i - u_o \right)^2 + \left( v_i - v_o \right)^2 - r^2 \\ &= \gamma_3 \left( u_i^2 + v_i^2 \right) + \gamma_2 u_i + \gamma_1 v_i + \gamma_0 \\ &= \Gamma^T X + \gamma_0 \end{aligned} \tag{5}$$

where $\Gamma^T = [\gamma_3 \quad \gamma_2 \quad \gamma_1]$ and $X^T = \left[ \left( u_i^2 + v_i^2 \right) \quad u_i \quad v_i \right]$. Assuming $u_o \approx 0, v_o \approx 0$, the best coefficient vector $\Gamma$ that minimizes the square error $\epsilon^2 = \sum \epsilon_i^2$ on the radius $r$ is given by:

$$\Gamma = \left( \sum X_i \, X_i^T \right)^{-1} \sum -X_i \tag{6}$$

These equations are valid under the following conditions:

- equation (6) is not ill-conditioned. This assumption is usually correct because enough data are distributed along the laser line profile during normal acquisition;
- outliers, i.e., point which creates an error $\epsilon > \epsilon_{max}$ are eliminated. These outliers are directly removed from equation (6) and a new set of coefficient $\Gamma$ is computed.

### *4.2. Ellipse*

It is also possible that an ellipse may best describe a non perfectly circular object by calculating the eccentricity of its shape. The surface of an ellipse, with major and minor axes $a$ and $b$, is $S = 1/4 \; \pi\sqrt{ab}$ and therefore $D_e = \sqrt{ab}$ becomes the equivalent diameter of the ellipse. The error equation, of centre $u_o, v_o$ and of unknown orientation $\theta$, becomes:

$$\epsilon_i = \gamma_5 u_i^2 + \gamma_4 v_i^2 + \gamma_3 u_i v_i + \gamma_2 u_i + \gamma_1 v_i + \gamma_0 \quad \textbf{(7)}$$

which is solved using $\Gamma^T = [\gamma_5 \quad \gamma_4 \quad \gamma_3 \quad \gamma_2 \quad \gamma_1]$ and $X^T = \left[u_i^2 \quad v_i^2 \quad u_i v_i \quad u_i \quad v_i\right]$ (equ. (6)).

## 5. Comparison with other methods: Compiled Scale and Back Projection

The compiled scale method is very similar to current practice of measuring the volume of wood using the 2-cm diameter class technique. Here the centre of the log is approximated using the best fit of a circle technique, then the longest and smallest segments between two opposite points are measured. The centre of the circle becomes the pivot of the search. The diameter is then calculated using $D_{cs} = \sqrt{ab}$. This method works only when multiple cameras (at least two) are used. In this paper, the 2-cm quantization effect was not included to compare the method at its best without introducing unwanted quantization errors.

Back-projection is equivalent to the technique used by some commercial systems. It basically consists of measuring the "shadow" of the object. Statistically, this technique assumes circular timber and, therefore, it can be affected by the orientation of the object and its exact shape. Furthermore, if the optical path is not perfectly parallel inside the working volume of the system, perspective effects can seriously alter the measurements. One technique consists of calculating the time interval of a scanning laser beam when the beam detects the log. Another method measures the size of the shadow of the log when it intercepts a plane of light. Good resolutions have been claimed but in practice these methods have a tendency to overestimate the volume. Using range data, this method is here implemented by calculating the diameter $D = \max(x_i) - \min(x_i)$ directly from the sensor data.

## 6. Volume measurement using raw data

Because the range sensor provides the *-u,-v* coordinates of several points on the profile of the object, exact cross-section can be calculated accurately and directly from the raw range data. This technique "naturally" includes the volume variations introduced by local deformations of the surface of the object that are normally rejected using simple geometrical models. This method should give an excellent estimate of the cross-section because it uses the exact profile of the object. Assuming *N* points on the profile and using linear interpolation between the points, the cross-section surface is directly computed using:

$$S = \frac{1}{2}\sum_{i=0}^{N-2}\left[\left(v_{i+1}+v_i\right)\left(u_{i+1}-u_i\right) + \left(v_0+v_{N-1}\right)\left(u_0-u_{N-1}\right)\right] \quad \textbf{(8)}$$

The method can be further improved, if sections are missing, by the use of more accurate interpolation techniques such as fitting arc segments on the range data or by more powerful numerical algorithms (e.g., Runge-Kutta).

## 8. Results

Table 3 shows the results for three different samples (logs) using the methods presented here. Several measurements have been done under different conditions, on each sample, to obtain all the possible views of the object. They are repeated using either one, two, or three cameras.

As expected, computed diameters using the raw data gives slightly better results than the other methods when the whole object is visible, and gives comparable results when a small section of the profile is missing. The algorithm is very stable. The best fit of an ellipse method should theoretically be better than the minimization of the circle. However, this is not so because of the five parameters to minimize, equation (7), making the algorithm more unstable than the three parameters for a circle , equation (5). Distortions and noise will have a greater influence. Finally, the errors associated with the two other methods are larger, as expected, especially for the back projection technique which clearly overestimates the diameter of the object.

| | | **Best fit of a circle** | | | **Best fit of an ellipse** | | | **Compiled Scale** | | | **Back Projection** | | | **Raw data** | | |
|---|---|---|---|---|---|---|---|---|---|---|---|---|---|---|---|---|
| | | Diameter | Errors | | Diameter | Errors | | Diameter | Errors | | Diameter | Errors | | Diameter | Errors | |
| | | Average (mm) | RMS % | Bias % | Average (mm) | RMS % | Bias % | Average (mm) | RMS % | Bias % | Average (mm) | RMS % | Bias % | Average (mm) | RMS % | Bias % |
| 3 | a | 179 | 0.2 | 0.1 | 179 | 0.4 | 0.01 | 179 | 0.8 | -0.3 | 184 | 2.5 | 5.2 | 179 | -0.4 | -0.2 |
| | b | 107 | 1 | 2.8 | 106 | 1.1 | 2.4 | 103 | 1.2 | -0.9 | 108 | 2.2 | 3.8 | 104 | 0.4 | 0.35 |
| | c | 299 | 0.1 | 0.3 | 298 | 0.3 | 0.1 | 293 | 1.2 | -5.4 | 303 | 10.9 | 4.5 | 298 | -0.1 | -0.03 |
| 2 | a | 179 | 1.1 | 0.2 | 181 | 1.6 | 0.9 | 178 | 2.4 | -0.5 | | | | 190 | 1.1 | 6.1 |
| | b | 107 | 1.8 | 3.5 | 110 | 5.6 | 6.4 | 104 | 2.8 | 0.3 | | | | 106 | 2.1 | 1.9 |
| | c | 300 | 2 | 0.6 | 303 | 4.7 | 1.7 | 298 | 6.5 | -0.5 | | | | 299 | 1.6 | 0.4 |
| 1 | a | 185 | 4.4 | 3.7 | | | | | | | | | | | | |
| | b | 127 | 28.8 | 22.8 | Unstable | | | | | | | | | | | |
| | c | 319 | 12.3 | 7.3 | | | | | | | | | | | | |
| | Sample | | | | | | | | | | | | | | | |
| Number of cameras | | | | | | | | | | | | | | | | |

**Table 3**: Comparison between different methods. Manual tape measurements are: a=179 mm, b=104 mm, c=298 mm.

## 9. Conclusion

The applicability of the Biris range sensor, for wood volume measurement, has been demonstrated using range data. The advantage of directly using range data to obtain accurate information on the cross section of timbers has resulted in simple processing algorithms to extract, in real-time, the desired information: volume, cross-section, and dimensions for each log.

Two methods have been shown and tested to measure the cross section of logs: 1) the fit of different models on the range data, and, 2) the direct measurement of the cross section from the raw range data. Although each technique has its advantages and disadvantages, some general observations can be made when processing "natural" objects:

- the fit of a model to the range data improves the robustness of the method, eliminating false measurements and outliers. However, selection of the proper model must be kept simple to reduce the number of unknown variables. Higher order models become quickly unstable and do not improve the quality of the measurements.
- Using raw data to evaluate the volume gives good results. The major source of error is introduced principally by the texture of "natural" object and their irregular shapes and, to a lesser extent, the accuracy of the measurements.

## 10. References

1. D.R. Phillips, M.A. Taras. "Accuracy of log volume estimates by density and formulas compared with water displacement." J. For. 31(10): 37–42; 1987.
2. V. Dove. "A non-technical discussion on the B.C. weight scaling system. Technical Conference on Wood Measurement Systems (Woodlands Section)", Québec, Que. Canadian Pulp and Paper Association, Montreal, Que., Canada, pp. E15–E20.
3. A.P. Kostiuk. "Sawmill scanners — scalers or process controller?" Tech. Conf. on Wood Measurement Systems (Woodlands Section), Québec, Que. Canadian Pulp and Paper Association, Montreal, Que. pp. E143–E147.
4. C. Myers and P.Yambert. "A Nu approach to measurement". J. For. 84(3): 44; 1986.
5. S.J. Potter. "Manager, forestry and engineering". Tech. Conf. on Wood Measurement Systems (Woodlands Section), Québec, Que. Canadian Pulp and Paper Association, Montreal, Que. p. E3.
6. F.Blais, M.Rioux, J.Domey. "Optical range image acquisition for the navigation of a mobile vehicle". Proc. of the IEEE Int. Conf. on Robotics & Automation, Sacramento, CA. April 9–11, 1991 Vol. 3. pp. 2574–2580.